Electronic Effects in the IR Spectrum of Water under Confinement†

Davide Donadio,*,‡ Giancarlo Cicero,§ Eric Schwegler,|| Manu Sharma,‡ and Giulia Galli‡

Department of Chemistry, University of California, One Shields Avenue, Davis, California 95616, Department of Materials Science and Chemical Eng., Politecnico di Torino, Turin, Italy, and Lawrence Livermore National Laboratory, Livermore, California 94550

Received: August 29, 2008; Revised Manuscript Received: November 18, 2008

We compare calculations of infrared (IR) spectra of water confined between nonpolar surfaces, obtained by molecular dynamics simulations with forces either computed using density functional theory or modeled by empirical potentials. Our study allows for the identification of important electronic effects, contributing to IR signals, that are not included in simulations based on empirical force fields, and cannot be extracted from the analysis of vibrational density of states. These effects originate from electronic charge fluctuations involving both surface and water molecules in close proximity of the interface. The implications of our findings for the interpretation of experimental data are discussed.

1. Introduction

Given the importance of confined water in a variety of scientific fields,[1] ranging from biology[2−5] to materials science,[6−8] many experimental and theoretical studies have been conducted to determine its properties. Many of these properties are, however, still the subject of debate.[9−12]

Interpreting experimental results on water in confined media has proven rather difficult in many instances, and firm conclusions based only on experimental observations are sometimes hard to draw. For this reason, it is desirable to interpret and complement experimental data by using atomistic simulations. Recently, we have undertaken a series of first-principles computational studies of the structural properties of water confined between hydrophilic silicon carbide surfaces[13] and nonpolar surfaces, including graphene sheets, carbon nanotubes,[14] and deuterated diamond.[15] For all cases, we found that the perturbation on the water hydrogen-bonded network induced by the confining surfaces is spatially localized within a thin interfacial layer (∼0.5 nm in the case of nonpolar substrates and slightly smaller, about 0.3 nm, in the case of SiC). An important question yet to be fully addressed is the identification of a set of observables allowing for a clear connection between simulations and existing and future measurements, thus providing a robust probe of the fluid under confinement.

Here, we focus on the vibrational properties of confined water, in particular its IR spectra. We compare results obtained using molecular dynamics (MD) simulations where the interatomic forces are either obtained by a parameter free approach based on density functional theory (DFT) or modeled through empirical potentials, and we discuss subtle but important electronic effects contributing to IR signals. Such effects can be accounted for only within an *ab initio* framework, and are responsible for specific features found in IR spectra. We chose to compare classical and first-principles calculations in the case of graphene, for which well established empirical interaction potentials are available in the literature. Our findings provide guidance in the interpretation of current and future experimental results, and highlight the importance of considering all contributions determining an IR signal, including electronic ones, and not only incomplete information contained in vibrational density of states. The comparison between IR spectra obtained with *ab initio* and classical calculations also sheds light on the nature of the interaction between water molecules and nonpolar confining surfaces.

The paper is organized as follows: in the next section, the theoretical framework of our classical and *ab initio* simulations is outlined, and the way we obtained IR spectra from equilibrium molecular dynamics simulations is described. In section 3, we discuss the *ab initio* results for water confined between graphene surfaces, and in section 4, we compare them to the spectra obtained from classical MD simulations. Section 5 contains our conclusions.

2. Method

We carried out MD simulations of water confined between graphene sheets at a distance of 1.01 nm, by using both a DFT treatment of the system[15] (hereon, we will refer to it as *ab initio* molecular dynamics, AIMD) and empirical potentials. In particular, we used a flexible simple point charge model (SPCF)[16] and a polarizable model.[17]

When performing computer simulations, the preparation of a solid/liquid interface within a confined medium is not straightforward. The main difficulty lies in estimating the number of water molecules required to fill up the confined space, in the presence of an excluded volume between the surface and the wetting layer. Such volume is not a priori known and eventually has to be subtracted from the volume accessible to water molecules, in order to determine the density of the confined fluid. To compute the number of water molecules, we determined the initial configuration of the system by using MD simulations with the SPC/E[18] potential in all cases. First, a trial system (with a tentative number of water molecules) was equilibrated and then MD runs were repeated either by changing the number of water molecules in the confined space or by varying the dimensions of the confining volume until the stress on the simulation cell corresponds to atmospheric pressure conditions. The samples obtained in this way were used as starting points for both *ab initio* and subsequent classical runs.

† Part of the special section "Aqueous Solutions and Their Interfaces".
‡ University of California.
§ Politecnico di Torino.
|| Lawrence Livermore National Laboratory.

10.1021/jp807709z CCC: $40.75
Published on Web 02/20/2009

We chose an SPC/E model to prepare our samples because well tested van der Waals parameters to describe the interaction between water and graphite surfaces and nanotubes (NTs) were available in the literature[19] and this model yields an equilibrium density of water similar to that obtained in DFT with the PBE[20] generalized gradient exchange and correlation functional.[21] In particular, the carbon atoms were modeled as neutral particles interacting with the oxygen atoms through a Lennard-Jones potential determined by the parameters $\varepsilon_{CO} = 0.3651$ kJ/mol and $\sigma_{CO} = 0.319$ nm.[19,22] In the graphene/water system, the cell dimensions in the (x,y) plane were fixed and determined by the size of a relaxed graphene sheet containing 60 carbon atoms (12.4 Å × 12.1 Å). In the z direction, the graphene layer distance was optimized to accommodate 32 water molecules. The carbon atoms of the graphite layer are free to move. The thickness of the exclusion volume present at the graphene/water interface, as determined by the atomic density profile $\rho(z)$, was estimated to be ~2 Å.

We performed MD simulations[23] to compute the IR spectra using two different parametrizations of the flexible SPC force field,[16,24] and a polarizable force field where the oxygen polarizability is described by a Drude model.[17] In these cases, the IR spectra were computed from the autocorrelation function of the total dipole moment $\vec{M}$, which is the sum of the molecular dipoles $\vec{\mu}_i$. The dipole of each water molecule for the flexible simple point charge (SPC) models used in the classical simulations is easily defined: $\vec{\mu}_i = q_O\vec{r}_O + q_H\vec{r}_{H1} + q_H\vec{r}_{H2}$.

In the first-principle MD simulations, the interatomic interactions are computed by solving the electronic structure within DFT using the generalized gradient approximation by Perdew, Burke, and Ernzerhof.[20] We adopted norm-conserving pseudopotentials,[25] and a plane-wave basis set with a cutoff of 85 Ry. In this case, we computed IR spectra using a version of Car−Parrinello (CP) *ab initio* MD,[26−28] in which maximally localized Wannier functions (MLWFs),[29] in place of Bloch orbitals, are propagated "on-the-fly". MLWFs are equivalent to Boys orbitals[30] used in quantum chemistry. Wannier functions (WFs) are obtained from the eigenstates of the Hamiltonian by a unitary transformation, and then MLWFs are derived from WFs by localization in real space. We use a time step of 7 au (0.17 fs) and a fictitious electron mass of 350 au to integrate the electronic and ionic equations of motion.[26] The main advantage of using MLWFs is that we can define the dipole moment of a water molecule μ_i as $\mu_i = e(\vec{r}_O + \vec{r}_{D_1} + \vec{r}_{D_2} - 2\sum_{l=1,4}\vec{r}_{W_l})$, where $\vec{r}_{D_1}$, $\vec{r}_{D_2}$, and $\vec{r}_O$ are the coordinates of the deuterium and oxygen atoms, respectively, and $\vec{r}_{W_l}$ are the centers of the four (doubly occupied) MLWFs associated to molecule i.[31−33] The total polarization is given as the sum of the individual dipole moments of the water molecules and the dipole moment of the surface atoms. The x and y components of the surface dipole have been computed from the atomic and Wannier center coordinates, modulo the "polarization quantum", as in the theory of polarization based on the Berry phase formalism.[34,35]

The IR absorption coefficient per unit length $\alpha(\omega)$ is related to the refractive index $n(\omega)$ and the imaginary part of the dielectric constant $\varepsilon(\omega)$ by $\alpha(\omega)n(\omega) = (\omega/c)\varepsilon(\omega)$. Within linear-response theory, $\alpha(\omega)$ is given by the power spectrum of the time-correlation function of the total dipole operator $\hat{M}$. Here, we approximate the quantum time-correlation function with the classical one, i.e., with $\langle M(0)M(t)\rangle$, where M is the total dipole moment in the simulation cell and the brackets indicate classical ensemble averages. The quantum time-correlation function can be expressed in several equivalent ways, leading to formulas for the IR absorption coefficient characterized by different prefactors; these are known as quantum correction factors. Following refs 36−38, we adopt the so-called harmonic approximation (HA) that is obtained by replacing the Kubo-transformed quantum correlation function with the classical one. The quantum corrected line shape $I(\omega)$ is

$$I(\omega) = \frac{\beta\hbar\omega}{1 - e^{-\beta\hbar\omega}} I_{cl}(\omega) \quad (1)$$

where β is the inverse temperature and $I_{cl}(\omega)$ is the Fourier transform of the classical $\langle M(0)M(t)\rangle$. In the harmonic regime, the HA is exact. Ramirez et al.[37] showed that HA is the only correction factor that satisfies the fluctuation−dissipation theorem in addition to detailed balance. The same authors also found that HA performs better than the other quantum correction factors for one-dimensional anharmonic potentials modeling several different H-bond scenarios. In ref 38, the HA prefactor was shown to provide a good agreement with experiment, for the relative intensities of IR absorption bands of deuterated bulk water computed within the same *ab initio* framework as in the present work.

In the HA, the IR absorption coefficient per unit path length of a sample of volume V is given by

$$\alpha(\omega)n(\omega) = \frac{2\pi\omega^2\beta}{3cV}\int_{-\infty}^{\infty} dt\, e^{-i\omega t}\left\langle \sum_{ij} \boldsymbol{\mu}_i(t)\cdot\boldsymbol{\mu}_j(0)\right\rangle \quad (2)$$

All of the IR and power spectra presented hereafter have been smoothened by a Fourier filter with a 50 cm^{-1} width.

The IR spectra have been computed in microcanonical (constant number of particles, volume and energy, NVE) MD simulations; the *ab initio* and classical runs were 10 and 50 ps long, respectively. Production runs were performed after equilibrating the system at 350 K[39] and at room temperature, in the *ab initio* and classical case, respectively.

The use of a CP scheme to perform *ab initio* MD involves assigning a fictitious mass to the electronic states (MLWF in our specific case) and a fictitious equation of motion for the electrons is solved at each ionic step, without solving self-consistently the Kohn−Sham (KS) problem. Values of this fictitious mass must be chosen carefully, for each specific system, in order not to affect significantly the dynamical properties of the simulated sample, and thus obtain results equivalent to those of Born−Oppenheimer (BO) simulations. In BO simulations at each ionic step, the electronic ground state is obtained by solving self-consistently the KS problem.[39] To check how the choice of the fictitious electronic mass affects calculations of IR spectra, we performed a CP simulation of a 16-molecule proton disordered model of hexagonal ice, with μ = 350 au, and we compared our results to those obtained by BO molecular dynamics simulations,[14,40] where the MLWFs were computed every 1.2 fs (Figure 1) using the algorithms developed in ref 41. We observed a red-shift of the spectrum computed by CP-MD, with the shift being larger, the higher the frequency. This shift depends on the inertial term introduced by the fictitious dynamics of the KS orbitals.[42] If the rigid ion approximation holds, for a monatomic system, it has been shown that the Car−Parrinello power spectra can be corrected by rescaling the CP frequencies (ν_{CP}) as $\nu = \nu_{CP}(1 + \Delta M/M)^{1/2}$, where M is the atomic mass and ΔM a correction proportional to the fictitious inertial term μ of the KS orbitals.[43] The

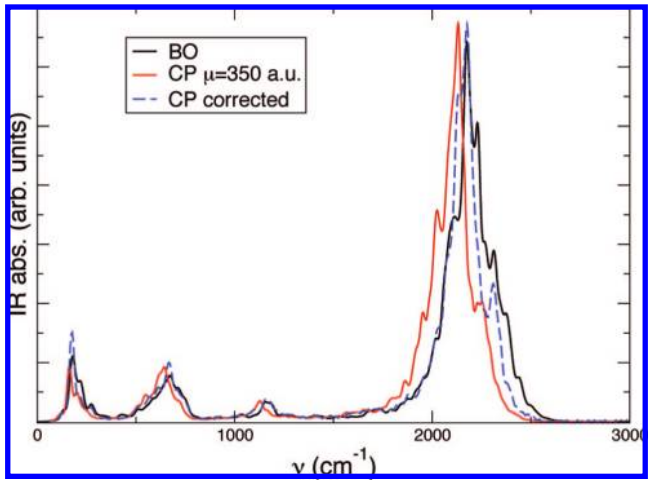

Figure 1. Simulated IR spectrum of deuterated ice I_h by Born−Oppenheimer (black solid line) and Car−Parrinello (red solid line) molecular dynamics with a fictitious electronic mass of $\mu = 350$ au. The IR spectrum obtained in a CP-MD simulation with the ionic masses rescaled according to ref 44 is also shown (blue dashed line).

correction cannot be applied *a posteriori* when more than one atom type is involved in the simulation, as in the present case, because different corrections apply to different atomic species. Therefore, the masses of the ions need to be corrected *a priori*. In Figure 1, we display also the IR spectrum of ice I_h obtained by a CP simulation with $\mu = 350$ au, with a mass correction based on the scaling factors reported in ref 44. The mass correction improves significantly the position of the peaks; however, the line shape remains qualitatively unaltered. Besides this frequency dependent shift, no significant changes have been observed in the IR line shape of ice computed with CP and BO simulations.

3. Ab Initio IR Spectra

In this section, we present the IR and power spectra of water confined by graphene sheets (composed of 60 C atoms) at a distance of 1.01 nm and discuss the main features of the IR signal arising from electronic effects. Before doing so, we briefly summarize the structural and electronic properties of the interfacial liquid layer.

The structural properties of confined water found in DFT-based MD simulations have been presented in refs 14 and 15, where it has been shown that, in the presence of a surface delimiting liquid water, density oscillations are induced extending a few angstroms from the interface, with an increased density of molecules in close proximity to the surface. In particular, close to a boundary, one or a few layers of water exist, which are structurally different from the bulk liquid. Interestingly, it has been found that the properties of this highly perturbed water layer do not depend on surface separation. In addition, even in the case of high, hydrophobic confinement, the perturbation on water structural properties induced by the surface is localized within a layer 0.3−0.5 nm thick. This is consistent with the results of recent investigations[45,46] where, based on experiments, upper bounds to the surface layer were given (varying between 0.25 and 0.6 nm).

It has been suggested[10] that a rarefaction of the density of water is present in proximity of a hydrophobic surface and this topic is still the subject of heated debate. Reference 10's results were recently challenged by Ocko et al.[11] and by Kashimoto et al.[12] Figure 2 shows the electronic and mass densities as a function of the z direction as obtained in our calculations. The

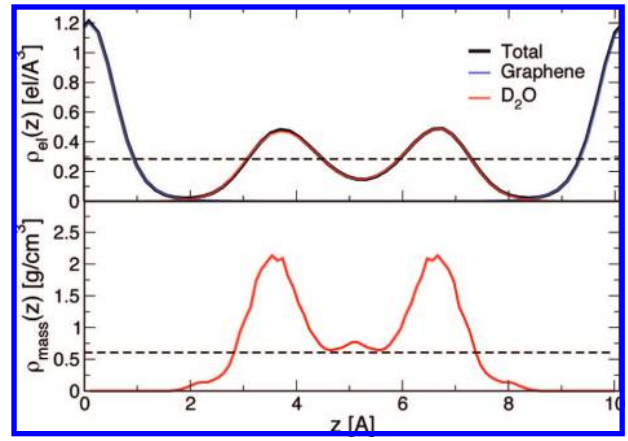

Figure 2. Electron (upper panel) and mass (lower panel) density of the coupled water−graphene system (32 water molecules confined within graphene sheets at a distance of 1.01 nm), as obtained from *ab initio* simulations (see text). The positions of the carbon atoms of the graphene layers are at 0 and 10.1 Å, respectively. The red, blue, and black curves represent the density of water, graphene, and the total density, respectively. The dashed line indicates the average electronic density in the bulk and the average mass density in the confined system, respectively.

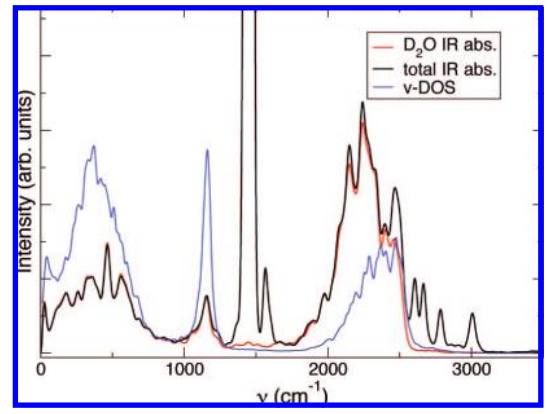

Figure 3. Computed IR spectrum of 32 D_2O molecules confined between graphene sheets at a distance of 1.01 nm. The black and red lines represent the full spectrum (D_2O plus surface) and that of the water molecules, respectively. The blue line represents the power spectrum of D_2O, obtained from the Fourier transform of the velocity autocorrelation functions of the D atoms.

observed depletion of electronic density in close proximity of the surface (i.e., in a region of linear dimension ∼1 Å from which water molecules are excluded) does not imply and is not accompanied by a rarefaction of water molecules at the interface. In fact, we find a peak of the mass density of water at the graphene interface, similar to that observed at the deuterated diamond interface,[15] showing the absence of a water molecule depletion layer, consistent with the results of ref 12.

In Figure 3, we report the computed IR spectrum of 32 water molecules in contact with graphene at a confinement of 1.01 nm (red line) and we compare it with computed vibrational density of states (v-DOS) (blue line) and with the IR signal obtained for the coupled water−graphene system (black line). The spectrum shown by the red line has been evaluated by restricting the sum yielding the total dipole moment to the water molecules only, when computing the dipole−dipole correlation function. The position of the lowest frequency peak and of the bending modes is the same in the v-DOS and IR spectra, although the relative peak intensities are different. The main peak of the high frequency modes is instead shifted toward

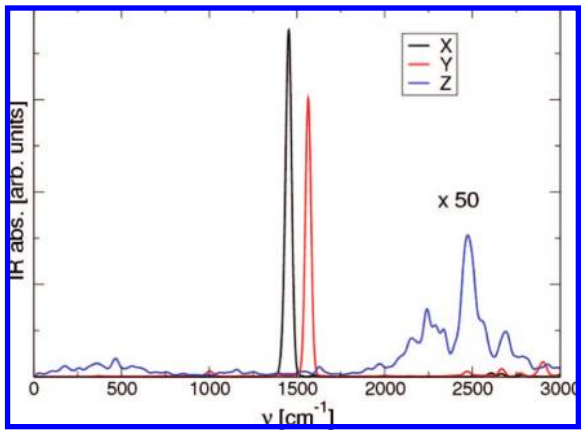

Figure 4. In-plane (*X*, black line; *Y*, red line) and out-of-plane (*Z*, blue line) contributions to the graphene sheet IR spectrum, originating from the oscillating dipole of the graphene foils. In the out-of-plane spectrum, a correlation with the IR modes of water can be seen by comparing with the results of Figure 3.

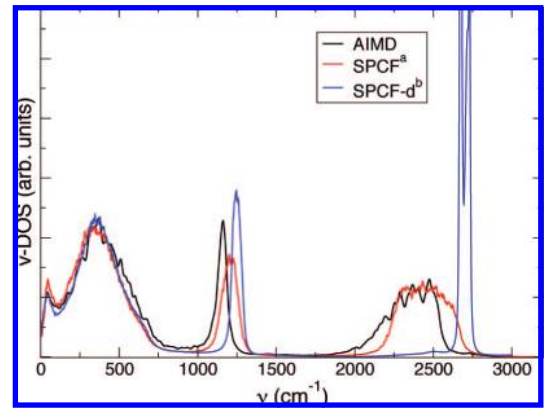

Figure 5. Comparison between the vibrational density of states (v-DOS) of confined water as obtained by using *ab initio* molecular dynamics (AIMD) simulations and two different flexible classical force fields: (a) SPCF;[16] (b) SPCF-d.[24]

higher frequencies in the v-DOS, compared to IR, indicating different IR activities of stretching modes, depending on whether or not OD bonds are engaged in hydrogen bonding and on the character of the hydrogen bonds (donor or acceptor). An analysis of the ionic trajectories shows that the peak of the v-DOS at 2500 cm^{-1} corresponds to OD bonds not engaged in hydrogen bonding with other molecules, and belonging to molecules in the immediate interfacial region. The feature corresponding to "free" OD bonds in the IR spectrum is much weaker than in the v-DOS, and it appears as a shoulder of the high frequency peak. This indicates that the IR activity of free OD bonds is negligible. This is surprising, as it is well-known that stretching modes of symmetric-top molecules such as water are IR active.

Interestingly, the full spectrum (surface plus D_2O), represented by the black line in Figure 3, does show a peak at ~2500 cm^{-1}. Therefore, the difference between the full spectrum and the D_2O spectrum must come from interactions between water molecules and the surface; indeed, we find that, in the case of interfacial water molecules, the electronic charge density fluctuations at the interface greatly affect the IR activity of O−D bonds not engaged in HB. In particular, it is the overlap of the highly polarizable p-electrons of graphene with the electronic charge density of the water molecules that is responsible for the modified IR activity. The intricate interactions of the electrons of graphene with the water molecules are also apparent when decomposing the IR spectrum of the graphene confining surface (Figure 4). The power spectrum of graphene shows no modes at a frequency higher than ~1600 cm^{-1}, while the IR spectrum reveals resonances with the IR modes of water.[15] The in-plane spectrum of the surface contains only a single mode (corresponding to the C−C stretch of the graphene layer); the out-of-plane spectrum contains instead a prominent peak at ~2500 cm^{-1}, and all of its features correlate well with those observed in the water−graphene spectrum. We emphasize that the high frequency peaks of the graphene spectrum are not related to ionic vibrations but to electronic charge fluctuations induced by the interaction with water.

These results show that an explicit treatment of the electronic structure of the surface and of the liquid is required to understand IR spectra and that interpretation of experimental results based solely on vibrational density of states (or power spectra) does not suffice and may be misleading.

It is interesting to note an analogy between the high frequency features observed in our simulated IR spectra and those reported for hydrogenated water confined in CNTs with very high curvature (diameter of ~1 nm).[9] The measurements of ref 9 have been interpreted as indicating the presence of a new phase of water under confinement, and in particular of weak interring bonds not present in the bulk. Our calculations show that a peak similar to that reported in ref 9 may appear due to charge fluctuations between the OD not involved in hydrogen bonds and the confining surface. Therefore, our results provide a possible, alternative interpretation of the data reported in ref 9. In fact, water tends to form small rings at hydrophobic (or weakly hydrophilic) surfaces, so as to maximize the number of hydrogen bonds, however without altering the local tetrahedral geometry[47] of the fluid. Although we observed the presence of an increased number of 4- and 5-fold membered rings in confined water, with respect to bulk water, we did not find the occurrence of quasi-planar structures in the interfacial fluid, as suggested in ref 9.

4. Classical MD Simulations

In the previous section, we have discussed the details of the IR spectra of confined water computed by AIMD simulations. In particular, we have shown that accounting explicitly for electronic polarization is essential to achieve a proper description of the interaction between graphene and water, and we have identified the fingerprints of such interaction in IR signals. In classical simulations, the surface water interaction is usually modeled by a Lennard-Jones potential[16,19] that does not include any specific information about the electronic structure of the confining surface, nor about the polarizability of the interfacial water molecules. Here, we aim at investigating the impact, on the description of IR spectra, of neglecting the water molecule polarizability, as done in several classical models, or of approximating it *via* a Drude model.

We compared the vibrational density of states obtained from simulations using two different parametrizations of the flexible SPC model,[16,24] and we conclude that the potential of refs 16 and 48 gives a satisfactory agreement with the power spectrum computed from first principles. In particular, Figure 5 shows that when using this potential there are no qualitative differences between classical MD and AIMD power spectra, except for a shift of the OD stretching and bending peaks. On the basis of our results for ice (see Figure 1), we ascribe these differences to inaccuracies of the *ab initio* IR spectra, introduced by the use of a fictitious electron mass in the AIMD simulations. While classical and *ab initio* v-DOS are qualitatively similar, the IR

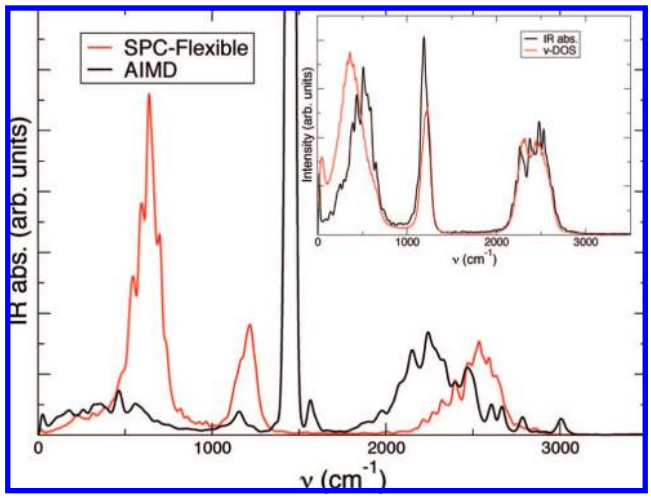

Figure 6. Comparison between IR spectra obtained by molecular dynamics simulations with classical potentials (red line) and by *ab initio* molecular dynamics (AIMD, black line) of water confined between two graphene sheets at a distance of 1.01 nm. The inset shows the power spectrum (v-DOS, red) and the IR spectrum (black) of bulk water from classical MD simulations adopting the SPCF force field.[16]

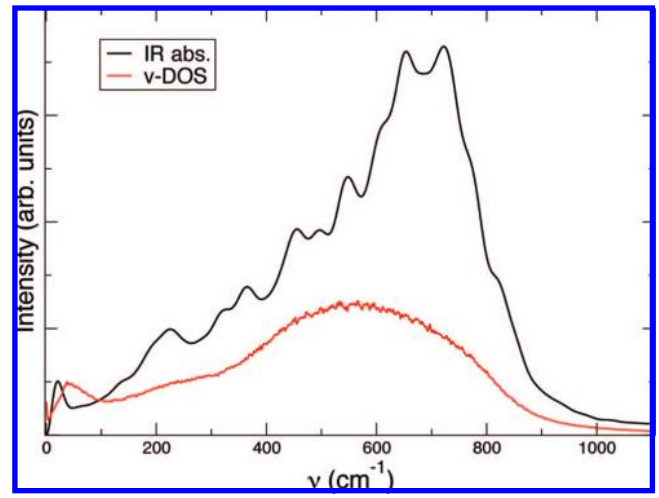

Figure 7. IR spectrum (black line) and vibrational density of states (red) of confined water from classical MD simulations with the polarizable SWM4-NDP potential.[17]

spectra obtained within the two formulations show very important differences both in peak position and relative intensities (see Figure 6).

As a classical potential does not account for dipole changes occurring in a water molecule upon rigid translation in a charged environment, the low frequency band related to hindered translations (ν less than 250 cm^{-1}) is absent in the classical IR spectrum. The hindered libration band is instead much amplified and is by far the most intense peak of the spectrum. This effect is strictly related to the fluid in the confined geometry, and it is much less prominent in the IR of bulk water obtained with the same classical potential (inset of Figure 6). The absence of a hindered translation band and the amplification of the hindered libration most likely stem from the unphysical lack of electrostatic coupling between water and the confining medium. In AIMD calculations, the hindered libration band is damped by polarization effects on given molecules, originating from surrounding water molecules; in a confined geometry, the intensity of this band is further damped by the polarization of the confining medium (graphene). Indeed, we have shown that the IR activity of graphene layers exhibit modes corresponding to all of the IR active modes of water (see Figure 4). The OD bending peak obtained in classical simulations is also more intense than in the AIMD spectra, again because of lack of polarization effects from the aqueous environment; in this case, the confining medium does not appear to play a significant role. The OD bending peak has similar relative intensity in the bulk and in the confined geometry; in addition, the corresponding out-of-plane component of the graphene signal, found in the *ab initio* simulation, is rather weak, indicating no substantial coupling between the water molecules and the electrons of graphene. In the high frequency OD stretching band, the mode related to non-hydrogen-bonded OD bonds does not appear as a distinct feature in the classical spectrum; however, a slight shift of the IR peak toward high frequencies with respect to the bulk is found.

From the comparison shown above, we conclude that even when using a flexible point charge potential yielding v-DOS in very good agreement with those obtained ab initio, the IR line shapes differ substantially from those found in first-principle calculations. This disagreement is due to the fact that classical model potentials do not account for water−surface interactions and polarization effects in a physically sound manner.

A possible route to incorporate polarization effects in a classical simulation is to use a polarizable Drude model. We therefore probed the IR spectrum of bulk and confined water, as described by the polarizable model by Lamoureux et al.[17] This model, dubbed SWM4-NDP, is built upon the TIP4P model.[49] The water molecules are treated as rigid bodies with fixed O−H length (0.9572 Å) and HOH angle (104.52°). A massless point charge is placed along the symmetry axis of the molecule in order to account for the permanent dipole moment of water. In addition to this TIP4P-like model, the SWM4-NDP force field has a charged shell associated to the oxygen atoms. The oxygen shell and core have opposite charges and therefore account for the effect of a varying dipole. As the water molecules are treated as rigid bodies, by using the SWM4-NDP model, we can only probe the far-infrared part of the spectrum, which is related to hindered translations and librations. The IR and power spectra of confined water are compared in Figure 7. At variance with the other classical models considered so far, hindered translational modes are found to be IR active, although the position of the peak in the IR spectrum is shifted with respect to the power spectrum. IR active translational modes have been previously observed for bulk water in ref 50, by using a classical polarizable force field; however, they differ from those found experimentally and by AIMD,[32] since they obey different selection rules. The ratio of the intensities of translational and librational modes is imbalanced in favor of the latter. This indicates that, as for the SPCF model, a screening term coming from the surface polarization is missing to attenuate the dipole fluctuations along the z axis. A possible reason is that only the water molecules are here treated as polarizable objects. Even if we cannot compare directly to the AIMD simulations, where also the polarizability of the graphene surface is fully accounted for, this result highlights the importance of considering explicitly the electronic effects on both the water and the confining medium.

5. Conclusions

In summary, we have presented a comparison between IR spectra of water confined within graphene layers, obtained by using *ab initio* and classical simulations. We have shown that, in order to describe the interaction of water with nonpolar

surfaces and to account for IR spectra, electronic charge density fluctuations occurring at the interface must be explicitly taken into account. In the near-IR region, *ab initio* vibrational and IR spectra show important differences arising from electronic effects, that is, electronic charge fluctuations occurring at the interface. We have also shown that, even in the case of classical potentials yielding v-DOS in good, qualitative agreement with *ab initio* results, computed classical and *ab initio* IR spectra differ substantially, due to the lack of a proper account of water−surface interaction and water polarization effects in classical simulations. The use of a polarizable Drude model for water brings classical and *ab initio* simulations into better qualitative agreement; however one should describe also the confining surface as a polarizable system to achieve a satisfactory description of the system.

Finally, our *ab initio* simulations show that all of the notable features found in IR spectra of water confined within graphene layers arise from mere interface effects, i.e., from interactions occurring in close proximity of the interface, and not from new phases of water under confinement.

Acknowledgment. We gratefully acknowledge support from Scidac Grant No. DE-FG02-06ER46262. Part of this work was performed under the auspices of the U.S. Dept. of Energy at the University of California/Lawrence Livermore National Laboratory under Contract No. DE-AC52-07NA27344.

References and Notes

(1) Buch, V.; Devlin, J. P. *Water in confining geometries*; Springer Series in cluster physics Springer: Berlin, 2003.
(2) Bryant, R. G. *Annu. Rev. Biophys. Biomol. Struct.* **1996**, *25*, 29.
(3) Israelachvilli, J.; Wennerstrom, H. *Nature* **1996**, *379*, 219.
(4) Balavoine, F.; Schultz, P.; Richard, C.; Mallouh, V.; Ebbesen, T. W.; Mioskowski, C. *Angew. Chem., Int. Ed.* **1999**, *38*, 1912.
(5) Nguyen, C. V.; Delzeit, L.; Cassell, A. M.; Li, J.; Han, J.; Meyyappan, M. *Nano Lett.* **2002**, *2*, 1079.
(6) Holt, J. K.; Park, H. G.; Wang, Y.; Stadermann, M.; Artyukhin, A. B.; Grigoropoulos, C. P. *Science* **2006**, *312*, 1034.
(7) Majumder, M.; Chopra, N.; Andrews, R.; Hinds, B. J. *Nature* **2005**, *438*, 44.
(8) Karaborni, S.; Smit, B.; Heidug, W.; Urai, J.; van Oort, E. *Science* **1996**, *271*, 1102.
(9) Byl, O.; Liu, J.-C.; Wang, Y.; Yim, W.-L.; Johnson, J. K.; Yates, J. T. *J. Am. Chem. Soc.* **2006**, *128*, 12090.
(10) Poynor, A.; Hong, L.; Robinson, I. K.; Granick, S.; Zhang, Z.; Fenter, P. A. *Phys. Rev. Lett.* **2006**, *97*, 266101.
(11) Ocko, B.; Dhinojwala, A.; Daillant, J. *Phys. Rev. Lett.* **2008**, *101*, 039601.
(12) Kashimoto, K.; Yoon, J.; Hou, B.; hao Chen, C.; Lin, B.; Aratono, M.; Takiue, T.; Schlossman, M. L. *Phys. Rev. Lett.* **2008**, *101*, 076102.
(13) Cicero, G.; Grossman, J. C.; Catellani, A.; Galli, G. *J. Am. Chem. Soc.* **2005**, *127*, 6830–6835.
(14) Cicero, G.; Grossman, J. C.; Schwegler, E.; Gygi, F.; Galli, G. *J. Am. Chem. Soc.* **2008**, *130*, 1871.
(15) Sharma, M.; Donadio, D.; Schwegler, E.; Galli, G. *Nano Lett.*, in press.
(16) M. C. Gordillo, G. N.; Marti, J. *J. Chem. Phys.* **2005**, *123*, 054707.
(17) Lamoureux, G.; MacKerell, A. D., Jr.; Roux, B. *J. Chem. Phys.* **2003**, *119*, 5185.
(18) Berendsen, H. J. C.; Grigera, J. R.; Straatsma, T. P. *J. Phys. Chem.* **1987**, *91*, 6269–6271.
(19) Werder, T.; Walther, J. H.; Jaffe, R.; Halicioglu, T.; Koumoutsakos, P. *J. Phys. Chem. B* **2003**, *107*, 1345–1352.
(20) Perdew, J. P.; Burke, K.; Ernzerhof, M. *Phys. Rev. Lett.* **1996**, *77*, 3865.
(21) McGrath, M. J.; Siepmann, J. I.; Kuo, I.-F. W.; Mundy, C. J. *Mol. Phys.* **2006**, *104*, 3619.
(22) Jaffe, R. L.; Gonnet, P.; Werder, T.; Walther, J. H.; Koumoutsakos, P. *Mol. Simul.* **2004**, *30*, 205–216.
(23) Smith, W.; Leslie, M.; Forester, T. R. *DLPOLY*, version 2.16; CCLRC, Daresbury Laboratoy, Daresbury, England.
(24) Deng, L. X.; Pettitt, B. M. *J. Chem. Phys.* **1987**, *91*, 3349.
(25) Hamann, D. R.; Schluter, M.; Chiang, C. *Phys. Rev. Lett.* **1979**, *43*, 1494.
(26) Car, R.; Parrinello, M. *Phys. Rev. Lett.* **1985**, *55*, 2471.
(27) Sharma, M.; Wu, Y.; Car, R. *Int. J. Quantum Chem.* **2003**, *95*, 821.
(28) http://www.quantumespresso.org.
(29) Marzari, N.; Vanderbilt, D. *Phys. Rev. B* **1997**, *56*, 12847.
(30) Boys, S. F. *Rev. Mod. Phys.* **1960**, *32*, 296.
(31) Gaigeot, M.; Sprik, M. *J. Phys. Chem. B* **2003**, *107*, 10344–10358.
(32) Sharma, M.; Resta, R.; Car, R. *Phys. Rev. Lett.* **2005**, *95*, 187401.
(33) Iftimie, R.; Tuckerman, M. E. *J. Chem. Phys.* **2005**, *122*, 214508.
(34) Resta, R. *Rev. Mod. Phys.* **1994**, *66*, 899.
(35) King-Simth, R.; Vanderbilt, D. *Phys. Rev. B* **1993**, *47*, 1651.
(36) Bader, J. S.; Berne, B. J. *J. Chem. Phys.* **1994**, *100*, 8359.
(37) Ramirez, R.; Lopez-Ciudad, T. L.; P, P. K.; Marx, D. *J. Chem. Phys.* **2004**, *121*, 3973.
(38) Chen, W.; Sharma, M.; Resta, R.; Galli, G.; Car, R. *Phys. Rev. B* **2008**, *77*, 245114.
(39) Grossman, J. C.; Schwegler, E.; Draeger, E. W.; Gygi, F.; Galli, G. *J. Chem. Phys.* **2004**, *120*, 300.
(40) Gygi, F. *QBOX*, version 1.33.3;http://eslab.ucdavis.edu/software/qbox.
(41) Gygi, F.; Fattebert, J. L.; Schwegler, E. *Comput. Phys. Commun.* **2003**, *155*, 1–6.
(42) Bloechl, P. E. *Phys. Rev. B* **1994**, *50*, 17953.
(43) Tangney, P.; Scandolo, S. *J. Chem. Phys.* **2002**, *116*, 14–24.
(44) Tangney, P. *J. Chem. Phys.* **2006**, *124*, 044111.
(45) Mezger, M.; Reichert, H.; Sch Schroeder, H.; Dosch, H.; Palms, D.; Ralston, J.; Honkimaki, V. *Proc. Natl. Acad. Sci. U.S.A.* **2006**, *103*, 18401.
(46) Ge, Z.; Cahill, D. G.; Braun, P. V. *Phys. Rev. Lett.* **2006**, *96*, 186101.
(47) Andreussi, O.; Donadio, D.; Parrinello, M.; Zewail, A. H. *Chem. Phys. Lett.* **2006**, *426*, 115–119.
(48) Marti, J.; Padro, J. A.; Guardia, E. *J. Mol. Liq.* **1994**, *62*, 17–31.
(49) Jorgensen, W. L.; Chandrasekhar, J.; Madura, J. F.; Impey, R. W.; Klein, M. L. *J. Chem. Phys.* **1983**, *79*, 926.
(50) Madden, P. A.; Impey, R. W. *Chem. Phys. Lett.* **1986**, *123*, 502.

JP807709Z